OPTICAL ELLIPSOMETRY ON THE DIFFRACTION ORDER OF SKINNED FIBERS

pH-Induced Rigor Effects

Y. YEH, R. J. BASKIN, K. BURTON, AND J. S. CHEN
Departments of Applied Science and Zoology, University of California, Davis, California 95616

ABSTRACT The polarization properties of light diffracted from single-skinned fibers of skeletal muscles have been examined under conditions in which the bathing solution pH and the ionic strength are changed. For fibers in the relaxed state, we observe large decreases in both the total depolarization signal, r, and the total diffraction birefringence signal, Δn_T, upon pH change from 7.0 to 8.0 at normal ionic strength. However, if the ionic strength is raised, then the r-value change as the pH changes from pH 7.0 to pH 8.0 is much smaller. If the rigor state is achieved at pH 8.0, and 0 mM ATP under either of the ionic strength conditions, the fiber can still be stretched. Rigor stiffness for this state is only ~20% that of the value of the stiffness at pH 7.0 rigor. Electron micrographs obtained under this pH 8.0 rigor state show that the overlap region can be decreased upon stretching the fiber, signifying a different kind of weaker-binding rigor state. Optically, the weaker-binding rigor state has a lower depolarization signal and larger form birefringence than the strong-binding rigor state. To convert from one type of rigor state (pH 7.0) to the other rigor state (pH 8.0), or vise versa, the fiber must first be relaxed. Apparently, either of the rigor states can block the full impact of the pH effect.

INTRODUCTION

Recent probe studies (1, 2) indicate that motion associated with the crossbridge during activation of skinned fibers is very much restricted. Based on these experiments and the time-resolved x-ray diffraction studies (3), Huxley and Kress (4) postulated that there may be two kinds of crossbridge binding during activation. In such a model, the strong-binding state is associated with most of the tension generation, whereas executing a relatively short stroke (~40 Å), the weaker-binding state may be considered a positioning state, preparing to make a transition over to the force-generating state. Although these activating states are not likely to be identical to the rigor state or the low ionic strength states (5, 6), the presence of two types of rigor states has also been suggested from the work of Taylor et al. (7). In the present study, optical ellipsometry has been used to characterize two distinct rigor states. The rigor state formed at normal pH (7.0) is a truly rigid state, whereas the rigor state achieved at high pH (8.15) is much weaker in binding. We shall correlate the optical ellipsometric findings with rigor stiffness and electron micrograph results.

Optical ellipsometry carried out on light diffracted into various orders from single fibers has been shown to contain much crossbridge information (8). In particular, we have shown that the myosin thick filament contributes significantly to the observed ellipsometry signals (9). The ability of this technique to, in principle, separate the contribution of intrinsically anisotropic elements from those isotropic elements contributing only because of their organized arrangements (form contribution) (10) has been suggested by us (11). In the present work, we will argue that in practice, the value of the depolarization ratio, r, is heavily weighted towards the intrinsic contribution. Using this technique of analysis, we discuss the change in the total ellipsometry signal as a single fiber is placed into rigor at different pH values. We will show that the rigor state at pH 7.0 is different from that at pH 8.15.

Myosin rods and fibers have been shown to exhibit a pH-induced phase transition (12, 13). Indeed the possibility that subfragment-2 (S-2) plays an active role in the contraction process has been suggested by Harrington (14), and since that initial paper, there have been several studies on the orientational freedom (15) and molecular conformations of S-2 and the myosin rod (16). The work of Reisler and Liu (17), and of Applegate and Reisler (18) on the myosin rods and minifilaments generally support the enzyme probe work of Ueno and Harrington (19–21), all suggesting that a region of the S-2-light meromyosin link is rather susceptible to enzymatic cleavage, particularly during activation (19) and upon bathing the molecules in a high pH (pH 8.5) buffer solution (20). The exact relationship of this pH-induced myosin rod change to the crossbridge contraction process, however, remains unresolved. Since the myosin rod has not been successfully labeled by extrinsic probes in its in situ state, the results reported here

represent data from a new diagnostic tool with which one can compare enzyme-probe results. Corroborative electron microscopic examination and stiffness tests of the single fiber under pH 7.0 rigor and pH 8.15 rigor conditions further support the idea that the actomyosin bond, even in the ATP-free state, can assume a strong or a weak bonding configuration depending on the pH of the solution.

MATERIALS AND METHODS

Sample Preparation

The lateral head of the anterior tibialis muscle from *Rana pipiens* was used in all experiments. A single fiber, after having been dissected in Ringer's solution, was soaked for 30 min in relaxing solution before skinning. This soaking eliminates the possibility of transient contracture when the fiber is in the skinning solution.

Skinning Procedure. The solution used for skinning the single fiber is the one described by us (22) previously, in which Triton X-100 is the active ingredient. The fiber is placed in the skinning solution for 15 min. After the skinning step, the fiber is returned to the relaxing solution. It was found that as long as a high concentration of EGTA was used in the solutions during these steps of the procedure, spontaneous activation in the relaxing solution could be minimized. As a result, 30 mM EGTA was used throughout these experiments. The specific compositions of all the solutions used in these experiments except at pH 5.5 and 6.0 are given in Table I, along with its pH and ionic strength conditions (23). Removal of the fiber from the skinning solution required care so that no excess skinning solution remained. The fiber was first placed in a relaxing solution with ATP. Repeated rinsing with fresh relaxing solution with ATP for a few minutes was necessary to rid the fiber of residual Triton X-100.

High Ionic Strength Buffer. We determined that if the relaxing solution is at normal ionic strength and high pH (solution 3), the relaxed fiber will still undergo spontaneous contraction waves for periods of up to 30 min even with high EGTA concentration (9). If the relaxing solution has high ionic strength (solution 4), then this contraction wave motion is abolished. Accordingly, we conducted most of the experiments under the conditions of high μ. The composition of these solutions is also listed in Table I.

Sample Placement. Aluminum foil clips were used to support the tendon region on either end of the fiber. The clips were mounted onto pins of the micromanipulator. The chamber that contained the fiber is bathed with relaxing solution that contained the desired pH, ionic strength, and ATP concentration. Each time the solution was changed, approximately 10 flushes were used. The sample chamber is maintained at 6°C by a flowing coolant that is thermostatically controlled by a constant temperature bath.

Sample Preparation for Electron Microscopic Measurements. Isolated single fibers were held at a preset sarcomere length in appropriate pH environments during fixation with 2% glutaraldehyde (in 0.275 M PIPES buffer). Sarcomere length was monitored during and after fixation to ensure that it remained constant. After a rinse in 0.3 M PIPES buffer (pH 7.25), fibers were postfixed in 1% osmium tetroxide (in 0.2 M PIPES, pH 7.25), rinsed, and placed in 70% acetone saturated with uranyl acetate. After serial dehydration in acetone, fibers were embedded and thin sectioned.

Stiffness Measurements. The method of measuring rigor state stiffness has previously been described by Yeh et al. (22). Skinned fibers were all held at a preset length (sarcomere length [SL] = 2.9 μm) for these experiments. The bathing solution was switched from relaxing to rigor, ensuring that the sarcomere length is preserved, and the sample cross-section was measured along two mutually perpendicular directions. A piezoelectric crystal was controllably displaced 0.8% of the total fiber length in 0.3 ms to simulate a step function drive. The transducer attached to the other end of the fiber records the stiffness and displays the result on an oscilloscope.

Method of Investigation

Preliminary Controls. All samples were first placed in the 4 mM ATP solution. This relaxing solution forms the base experimental condition. The length of the fiber is determined by micromanipulator positioning and the sarcomere length is measured by the position of the first optical diffraction maximum. Even though the general quality of the skinned fiber has already been checked by a stereomicroscope during the fiber mounting stage, the uniformity of the fiber in terms of quality for experiments is found to be best evaluated by taking ellipsometric measurements over a large section (1 mm) of the length of the fiber at close spatial intervals (100 μm). If the fiber exhibited good reproducible ellipsometric parameters over these regions, then the experiments can proceed. Otherwise, only a limited set of experiments that do not compromise the integrity of the fiber can be conducted.

The Ellipsometer. For these quasistatic experiments, the technique of quarter-wave plate rotation provided the unambiguous

TABLE I
SOLUTIONS USED IN THESE STUDIES

No.	pH	μ	KCl	Imidazole	Tricine	EGTA	$MgCl_2$	Na_2ATP	HCl	KOH
			Relaxing solutions							
1	7.0	140	24.66	9.6	—	28.8	1.3	4	1.9	—
2	7.0	216	96.0	9.6	—	28.8	0.96	4	1.9	—
3	8.0	177	24.66	—	9.6	28.8	1.26	4	—	6.7
4	8.15	257	96.0	—	9.6	28.8	0.96	4	—	11.5
			Rigor solutions							
5	7.0	115	25.7	10.0	—	30.0	1.3	—	2.0	—
6	7.0	193	100.0	10.0	—	30.0	1.0	—	2.0	—
7	8.0	163	25.7	—	10.0	30.0	1.3	—	—	7.0
8	8.15	244	100.0	—	10.0	30.0	1.0	—	—	12.0

All concentrations are in millimolars.

ellipsometric parameters with good signal-to-noise ratios. The apparatus was described in a previous publication in some detail (24). Briefly, a polarized He-Ne laser with its plane of polarization at 45° relative to the fiber axis impinges upon the fiber at normal incidence. The detection arm contains the stepping-motor driven rotating quarter-wave plate, an analyzing polarizer set at 0°, and a photomultiplier tube (PMT). Both the digitized stepping-motor position signal and the PMT pulse signals are fed into a Digital Equipment Corp. (Marlboro, MA) LSI/11-23 microcomputer for data processing and analysis. A nonlinear least-square fitting of the experimental curve leads to the determination of the ellipsometric parameters: the total birefringence on the diffraction signal, $D n_T$, and the depolarization amplitude, r. In all of these experiments, both the amplitudes and the phase angle of the elliptically polarized diffracted light are measured. The observed phase angle, δ, is converted into a total birefringence value, Δn_T, by the equation

$$\Delta n_T = \frac{\delta \lambda_0}{2\pi d}, \tag{1}$$

where λ_0 is the wavelength of light in vacuum, and d is the thickness of the traversal distance which, in these experiments, is taken to be the thickness of the fiber. A principal element of these investigations is that even though there is, theoretically, a coupling of the intrinsic and form contributions in the measured parameters, the weighting of the respective parts is substantially different. Whereas the total birefringence, Δn_T, depends on the total matter traversed by the light, whether forward or on the diffraction order, the total depolarization value, r, on the diffraction order, however, vanishes if A-band and I-band do not differ in their dielectric constants. This fact results in a normalization factor proportional to the differential indices of refraction for the intrinsic part of r, while the form part of r still requires the presence of the entire matter-solvent refractive indices difference. Since the normalization factor enters in the denominator of r, the result is an enhancement of the intrinsic part of r. In our unpublished analysis, we show that a 50%-50% weighting of the birefringence contributions between the two components leads to a 90%-10% weighting of the intrinsic to the form contribution in the r-value evaluation. Consequently, for a first approximation we will assume that the observed r-value reflects mostly intrinsic contribution. The two intrinsic polarizabilities, α_1 and α_2 of the fiber leading to the observed elliptically polarized diffracted signal, are used in the equation

$$r = \left| \frac{\alpha_1 - \alpha_2}{\alpha_1 + \alpha_2} \right| \tag{2}$$

for an evaluation of the intrinsic depolarization, r, of this diffraction system, normalized to be rid of the influence of source intensity variation.

The Form Contribution

Irving (25) has recently reported on the transmission birefringence studies of active fibers undergoing isometric contraction. He attributed the changes in birefringence in those studies to movement of the subfragment 1 (S-1) moieties. Studies of muscle birefringence (26, 27) point to the fact that two contributions to such data exist. Not only do ordered isotropic elements exhibit form birefringence, but intrinsically anisotropic elements will provide an intrinsic contribution. As discussed in the above section, from the diffraction ellipsometry data we can begin to separate the contributions because both r and Δn_T data are available to us. Since the intrinsic contribution is, to a large extent, a property of the r data, we have developed an analytical method to subtract the measured change of intrinsic contribution resulting from an imposed chemical change from the total measured birefringence change. This difference, $d\Delta n_F$, corresponds to an evaluation of the form contribution alone:

$$d\Delta n_F = d\Delta n_T - d\Delta n_I. \tag{3}$$

However, since Δn_T and Δn_I are obtained from different parts of the ellipsometric data, the normalization we used is the relative change upon chemical change of state, not the absolute change. Since the change in r-value is assumed to be proportional to the change in intrinsic birefringence, we have $(d\Delta n_I/\Delta n_I) \propto (dr/r)$. The equation with which we extract the form contribution is given by

$$(\Delta n_F)_1 = \left[1 + \left(\frac{d\Delta n_F}{\Delta n_F}\right)_0\right]\left(\frac{\Delta n_F}{\Delta n_T}\right)_0 (\Delta n_T)_0 \tag{4}$$

where

$$\left(\frac{d\Delta n_F}{\Delta n_F}\right)_0 = \left(\frac{\Delta n_T}{\Delta n_F}\right)_0 \left\{\left(\frac{d\Delta n_T}{\Delta n_T}\right)_0 - \left[1 - \left(\frac{\Delta n_F}{\Delta n_T}\right)_0\right]\left(\frac{dr}{r}\right)_0\right\}, \tag{5}$$

and where the subscript F denotes form contribution. The subscript 0 denotes the initial state conditions, whereas the subscript 1 denotes state after a chemical state change has taken place. The notation $(dx/x) = (x_1 - x_0)/x_0$, where $x = \{\Delta n_T, r, \Delta n_F\}$. These equations (Eqs. 3–5) are self-propagating in the sense that all subsequent Δn_F values can be calculated from the measured values of r and Δn_T once an initial assumption of the initial state form-to-total birefringence ratio is made. We have assumed that for the initial state of each fiber, the value of $(\Delta n_F/\Delta n_T) = 1/2$. The subsequent values of form birefringence change upon pH change are calculated according to Eq. 4, where the ratio of form-to-total contribution is allowed to vary accordingly. It is clear that the derived Δn_F values are dependent upon the initial assumption of the value of $(\Delta n_F/\Delta n_T)$. As will be shown later, the value of 1/2 for sarcomere length of 2.9 μm provided us with an assumption that is self-consistent with experimental results.

RESULTS

Relaxed Fiber, pH Variation from 5.5 to 8.5

It is well known that the fiber lattice is sensitive to the presence of ions in solution (6, 28). Changes in ionic strength and changes in the pH of the solution both lead to changes of the lattice dimension. In the low ionic strength case, this effect is due to an increase in charge repulsion upon a decrease of counterion concentration. For the high pH case, charge repulsion is due to an increase in the number of exposed charges on the proteins. Thus the expected lattice change upon pH change is a proportional one: The lattice is compressed at low pH (pH 5.5) and becomes expanded at pH 8.5. Upon lattice change, the relaxed fiber will certainly exhibit changes in the form birefringence, while any related orientational freedom change of the anisotropic elements will also modify the intrinsic contribution of the birefringence as well as the depolarization ratio, r. In our previous publication (9), we showed that for the relaxed fiber, the change in lattice upon pH change is small. In Fig. 1, both Δn_T and r of a representative single fiber are plotted against the pH of the solution. The most notable point of this figure is the rapid, sigmoidal shaped decrease of r and a corresponding decrease in Δn_T when pH varied from 7.0 to 8.0. The error bars shown represent the repeatability of the data for that same fiber. Table II exhibits the averaged values of eight fibers, each of which gave similar results in terms of relative changes of r and Δn_T. Overall, the averaged

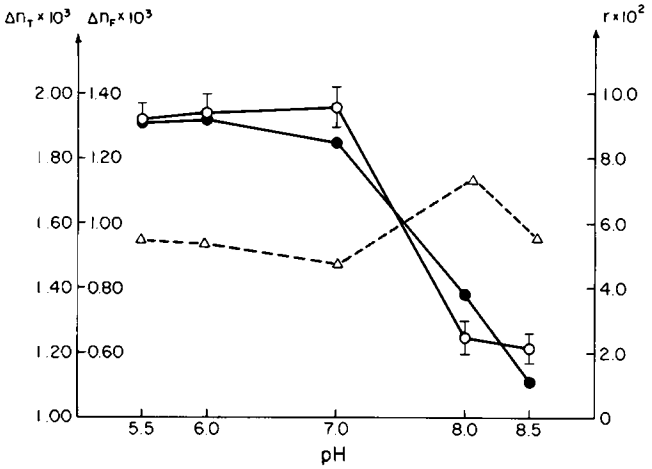

FIGURE 1 Measured changes in Δn_T (*solid circles*) and r (*open circles*) upon pH change from pH 5.5 to 8.5 in relaxing solutions at normal ionic strengths. *Open triangles*, calculated Δn_F from Eq. 4 assuming initially $\Delta n_F/\Delta n_T = 1/2$. SL ~ 2.9 μm.

change of r from pH 6.0 to 7.0 is ~ −7%, whereas from pH 7.0 to 8.0 the change is nearly −50%. Also plotted in Fig. 1 are the calculated Δn_F values assuming that at pH 5.5 and 4 mM ATP concentration, $\Delta n_F/\Delta n_T = 1/2$, and using Eqs. 4 and 5. The calculated increase in Δn_F is +12.5% from pH 6.0 to 7.0 while over the pH range of 7.0 to 8.0, the increase is +20.6%. Although the standard deviation in this Δn_F calculation is rather large, the numbers do reflect a systematic increase in the form part of birefringence. Since the values of r reflect approximately the changes in the anisotropic elements alone, we may interpret the initial change (pH 5.5 to 7.0) and the final change (pH 8.0 to 8.5) to be the gradual opening up of the lattice and therefore there is more space for the anisotropic elements, perhaps S-2, to orient more freely and decrease the effective optical anisotropy. Over the range of pH from 7.0 to 8.0, however, the slopes of curves are much larger, suggesting that perhaps there is another mode of altering the depolarization ratio besides orientational change. Since at this ionic strength, we always noticed contraction waves as soon as the solution is at the high pH 8.15 condition, we could interpret this large signal change as resulting from residual spontaneous activation of the fiber system, even though we wait for the contraction waves to damp out before taking data. Concomitant with the rapid decrease in r, there is a rise in the form birefringence. Such a behavior has been observed in activation experiments (29), where a decrease in r may be interpreted as being due to the anisotropic element tilting upward, and the increase in Δn_F is caused by isotropic elements redistributing its average mass concentration. To minimize this activation effect we used high ionic strength relaxing solution, where the decrease in r upon pH increase to 8.15 is much less and the increase in form birefringence likewise remains small (Table II). However, if the ionic strength of the relaxing solution at high pH is then decreased to normal strength, the dramatic decrease in r and increase in Δn_F is again observed. This effect is shown for one of our nine experiments conducted under these conditions (Fig. 2). Invariably this step is associated with visible contraction waves that persist for nearly 20 min.

TABLE II
AVERAGED RELATIVE PERCENT (%) CHANGE IN r AND Δn_F FOR RELAXED FIBER UNDERGOING pH CHANGES

	pH 6 → pH 7 (8)	pH 7 → pH 8	
		Normal μ (8)	High μ (9)
$\frac{dr}{r}$	−7.7 ± 8.5	−50.1 ± 19.8	−8.7 ± 3.7
$\frac{d\Delta n_F}{\Delta n_F}$	+12.5 ± 10.1	+20.6 ± 16.8	+6.6 ± 3.9

Normal μ refers to solutions similar to 1 and 3 of Table I, while high μ refers to solutions 2 and 4. Numbers in parentheses correspond to the total number of fibers examined in that average. + or − values correspond to standard errors.

Rigor States upon pH Variation from 5.5 to 8.5

The rigor state is characterized by well-defined angle or angles of orientation between the S-1 and actin filament (7), and furthermore, the bond between S-1 and actin is rigid. If the fiber is initially placed in the rigor state at low pH (5.5), and then the pH of the solution is increased to a value of 8.5 while still maintaining 0 mM ATP, we find that (Fig. 3 *a*) the r values increased by 24% while Δn_T decreased by almost 25%. The calculated Δn_F correspondingly decreased. If, on the other hand, the rigor state is approached by first placing the fiber in the relaxed pH 8.5 solution and then removing the ATP, this new rigor state

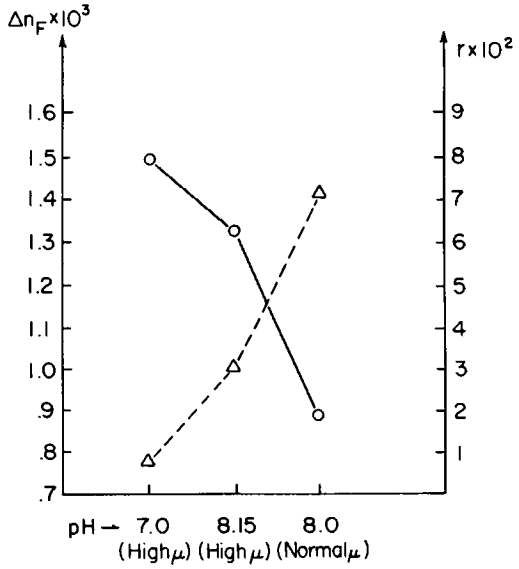

FIGURE 2 Measured changes in Δn_T (*open circles*) and r (*open circles*) upon pH and μ change in relaxing solutions. *Open triangles*, calculated Δn_F. SL ~ 2.9 μm.

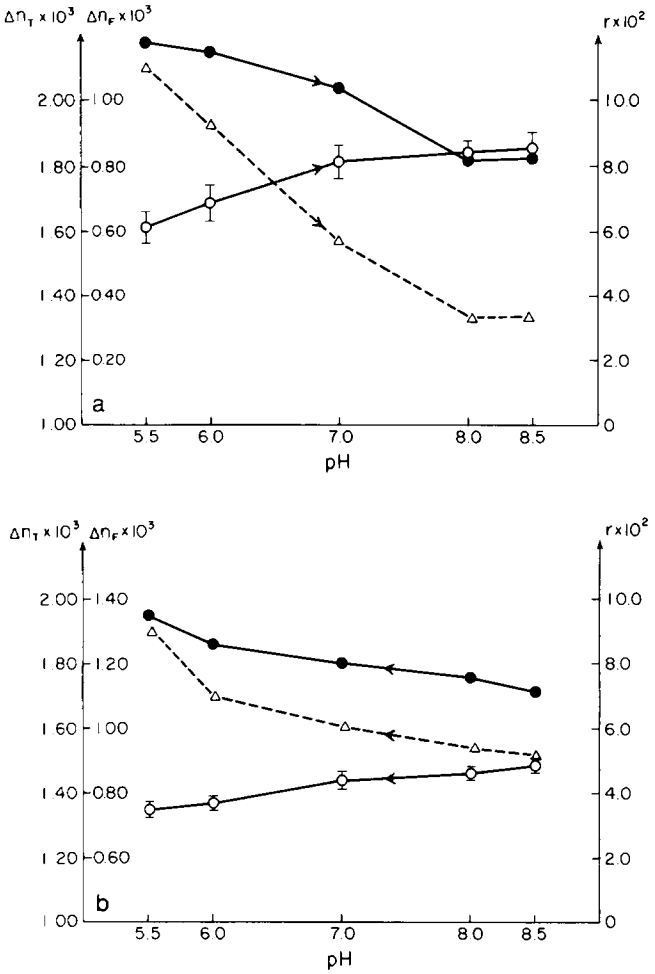

FIGURE 3 Measured changes in Δn_T (*solid circles*), r (*open circles*), and calculated changes in Δn_F (*open triangles*) for fiber in rigor solution. (*a*) Initiating from the low pH true rigor state. SL = 2.9 μm. (*b*) Initiating from the high pH pseudo-rigor state. SL = 2.9 μm.

has some interesting properties. The optical signals, r and Δn_T at pH 8.0, are both substantially lower than the values of the rigor state at the same pH, but reached via the rigor pH 7.0 state. If the pH is changed while maintaining this rigor state, the optical signals at corresponding pH values are likewise lower (Fig. 3 *b*). The trend of change in the calculated values of Δn_F remains similar. This result suggests that the rigor state attained from the lower pH values is not the same state as that rigor state attained from pH 8.5. Once in this lower rigor state, three mechanical features are noticed: (*a*) The fiber can still be stretched. The extension can easily amount to 10% of its original length although for certain fibers with initial length set at 2.9 μm a stretch of 30–40% can be achieved. (*b*) The fiber cannot be contracted below its original length. (*c*) The stiffness of the fiber in the pH 8 rigor is significantly less than those in the pH 7 rigor fiber. Four fibers were each held at SL = 2.9 μm. Upon the 0.8% stretch, stiffness of the two pH 7 rigor fibers measured were 3.31 and 2.55 N/m. On the other hand the stiffness of the two pH 8 rigor fibers were 0.67 and 0.70 N/m. We labeled this pH 8 rigor state the "pseudo-rigor" state. This stretchable pseudo-rigor state suggests that (*a*) there may be an extremely elastic element associated with this state, (*b*) the high pH rigor state does not allow for the establishment of strong actomyosin bonds such as those of the true rigor states, or (*c*) there are fewer bonds in the pH 8 rigor state. We therefore conducted electron microscopic studies of the fiber in pH 8.15, 0 mM ATP solution after the stretch had been effected. For comparison, an electron micrograph of an unstretched fiber in pH 8.15 rigor solution is given. We see from Fig. 4 that in this high pH rigor state (Fig. 4 *b*), the stretch resulted in a decrease of the thick and thin filament overlap. In the meantime, the length of the f-actin and the myosin filaments is essentially the same as that of the same sample at pH 7.0 (Fig. 4 *a*). This result suggests that there is little elastic compliance in the high pH rigor fiber; however, the number of actomyosin bonds or the strength of bonds must still be resolved.

One test is the lattice spacing experiment. To more closely examine the fiber diameter change upon entering rigor in these two states, four fibers were each subjected to pH 7 relaxed-rigor state changes, followed by pH 8 relaxed-rigor condition changes, taking due precautions of the rigor state hysteresis to be discussed below. From our data, there is little expansion detected in the relaxed state upon going from pH 7 to 8.

In Table III, the tabulated values at the listed pH and sarcomere length conditions are obtained from the expression for average fiber size given by $s \sim \sqrt{(w \cdot d)}$, where w is the measured diameter of the fiber and d is the fiber depth measured by the 45° mirror-microscope system. It is further assumed that the lattice spacing is directly proportional to this parameter, s. We measured s for the fiber in relaxed pH 7, rigor pH 7, relaxed pH 8, and pseudo-rigor pH 8 conditions. Upon entering the rigor states, pH 7 rigor solution generally does not alter the lattice diameter significantly, whereas pH 8 rigor solution always decreases the fiber diameter.

This result differs from the study reported by Matsubara et al. (30), in that they observed a small but consistent decrease in lattice spacing upon entering into rigor at pH 7. There are two major differences between our experiment and those of Matsubara et al. First, our fibers were chemically skinned, whereas their fibers were mechanically skinned. A recent study by Higuchi and Umazume (31) supports the idea that mechanically skinned fibers differ in elastic properties from chemically skinned fibers. Second, the sarcomere length was kept constant in our experiment by using the pH 7 rigor state as the reference state. Upon relaxing the fiber at pH 7, the accompanying change in sarcomere length was compensated before these diameter measurements were made. Since both of the pH 8 states were non-stiff states, the sarcomere lengths were again adjusted after each solution change. Thus stiffness was actually lower in the pseudo-rigor state, a state that has a lattice spacing less than that of the pH 7 rigor state.

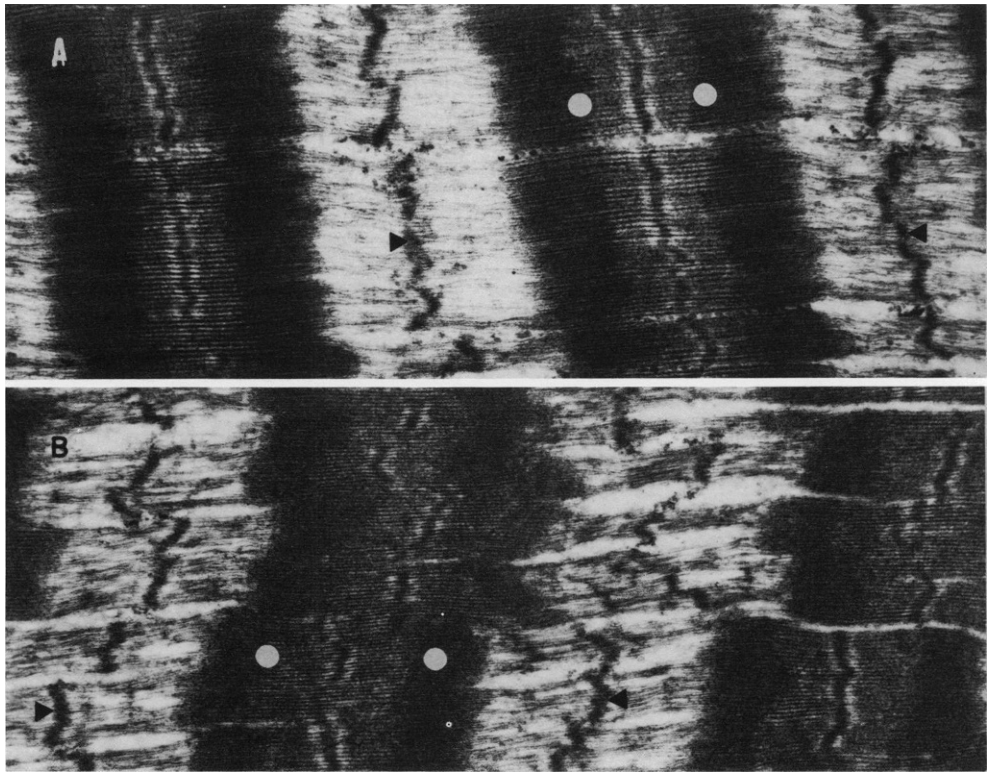

FIGURE 4 Electron micrographs of pseudo-rigor fiber fixed at pH 8.15. (*A*) SL = 2.81 μm. (*B*) Stretched to SL = 3.46 μm. Distance between the dots marks the bare zone of the A-band. Note that the dark total A-band region as well as the I-band distance between dot and Z-line are essentially unchanged in length while the bare zone increased upon stretch.

Such a result is inconsistent with a decreased number of crossbridges in the pseudo-rigor state.

We also note that decreasing pH in this state of pseudo-rigor cannot cause the fiber to enter into the true rigor state. The inability to start from one rigor state and attain the other rigor state directly by a pH change alone suggests two possibilities: There may be a pH-related molecular phase transition occurring in the relaxed state for the fiber to enter into the other rigor state. On the other hand, either of the rigor states may be able to shield the crossbridge system from the true pH environments, which, if effective, would lead to the two different rigor states.

Rigor State Hysteresis

In a series of studies designed to test the specific step where reversibility of the observed changes can take place upon pH changes, we used two different protocols: (*a*) The fiber is initially placed in the pH 7.0, 4 mM ATP state. After the solution pH is changed to 8.15, ellipsometry data are obtained. Then the fiber is returned to the pH 7.0 relaxing solution. This process is repeated for several cycles. We find the reversibility of the optical signals upon solution reversal to be essentially complete. Furthermore, the changes in r and Δn_F are consistent with other values in Table II, obtained at the high pH condition.

(*b*) Having shown that the elementary steps associated with the relaxed fiber, initially in the pH 7.0 relaxed state, *A* is put into conventional rigor *B*. Then rigor at pH 8.5 is achieved without first re-relaxing the fiber *C*. At this stage, the fiber remains in the true rigor state. The fiber is then relaxed at pH 8.15 (*D*). The removal of ATP in this high pH condition results in the fiber entering the pseudo-rigor state, as indicated by the optical data of points labeled (*E*), and by the presence of mechanical compliance much greater than that of the true rigor state. While in this pseudo-rigor state, the system is returned to pH 7.0 (*F*) where basically the optical and mechanical responses still reflect that of the pseudo-rigor condition. Finally this state is relaxed (*G*), recovering the conditions of *A*. If the transition is indeed reversible, the values of states *A* and *G* should be identical. Fig. 5 *a* shows that indeed the r-value is

TABLE III
AVERAGE FIBER DIMENSIONS IN MICRONS (μ) UNDER THE CONDITIONS OF pH CHANGE AT FOUR SARCOMERE LENGTHS

Fiber SL	Relax pH 7	Rigor pH 7	Relax pH 8	Pseudo-rigor pH 8
2.60	75.2	78.3	78.1	67.1
2.66	79.5	80.1	76.9	73.8
2.93	65.7	63.1	66.4	59.5
3.30	65.7	66.6	66.1	61.6

This parameter, s, is calculated from the width and depth measurements using a microscope with a Filar eyepiece (see text).

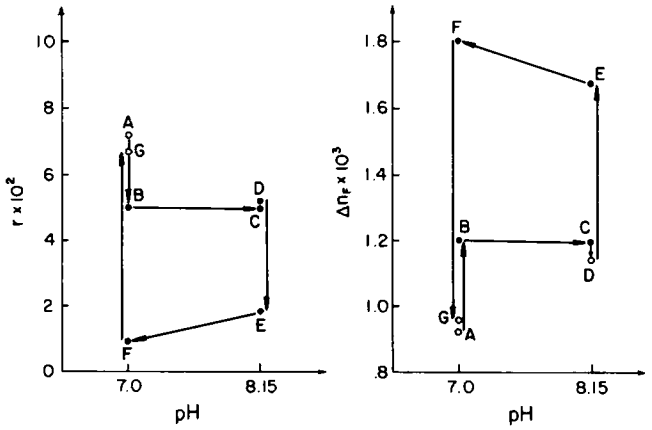

FIGURE 5 Hysteresis loops in r and Δn_F upon changes in the solution bathing the fiber. Δn_F is calculated from Δn_T and r values using Eq. 4. The states are labeled *A–G* (see text). SL = 2.9 μm.

reversible. Not shown in the figure is the result that Δn_T is also fully reversible. As a consequence, we chose the appropriate $(\Delta n_F/\Delta n_T)_0$ ratio to render Δn_F reversible as well. This parameter fitting technique using Eqs. 4 and 5 led us to use $(\Delta n_F/\Delta n_T)_0 = 0.5$ for the most complete reversibility of Δn_F. Using initial $\Delta n_F/\Delta n_T$ values of 0.4 or 0.6 led to substantial disagreement between the final value of Δn_F in *G* and the initial value in state *A*.

As an added test of the existence of this pseudo-rigor state, we conducted the same loop experiment at the full-overlap (SL = 2.4 μm). The results are fully consistent with our data at SL = 2.9 mm. The repeatability at this sarcomere length condition suggests that pseudo-rigor is not a state whereby the end elements of the myosin thick filament has started to fray, thus leaving a weaker resulting structure because the number of bonds is much reduced.

DISCUSSION

Two Distinct Rigor States

This series of experiments has shown that two types of rigor states can be discerned when the pH of the bathing solution is allowed to change from pH 7.0 to 8.15 or above. The rigor state entered into at the lower pH values is the state with a tight-binding actomyosin complex. This is the normally encountered rigor state, which we have called the true rigor state. Mechanically, the state is characterized by high stiffness: The fiber cannot be extended or contracted. Optically, the depolarization ratio, r, decreases a small amount from its relaxed state at the corresponding sarcomere length. At the same time, there is a small increase in the form birefringence signal, Δn_F. To relate these changes to models of the crossbridge structure, we first discuss the implications of either intrinsic or form change.

Changes in the intrinsic anisotropy can come about from either changes of the molecular structure so that the magnitude of the intrinsic anisotropy is changed, or of the orientation of the anisotropic element as presented to the incident electric field. Form anisotropy is defined by the effective difference of indices of refraction along the two polarization directions of the incident field due to different ordering of isotropic elements along those directions (9). Along the fiber axis, we can assume that the index of refraction is a constant, reflecting the averaged index of refraction of the large number of thick and thin filaments spaced by some solvent medium. The differences in the indices of refraction between the thick and thin elements along the fiber axis contribute primarily to the observed diffraction patterns. Our experiments show no appreciable change in sarcomere length upon changing the solution conditions. On the other hand, the transverse direction to the fiber axis is the direction where most of the crossbridge movements take place. The shifting of mass elements such as S-1 from the thick filament towards the thin filament will cause a redistribution of the average dimension of the regions with and without fiber elements. Since form birefringence depends on both volume fraction and the shape of the arranged elements, changes in either will reflect form birefringence change. We measured a nearly 10% decrease in the lattice spacing upon entering into the pH 8 psuedo-rigor state; however, the form birefringence increase is not 100%. This is likely due to effective shape changes of the thick filaments associated with the crossbridge movements.

In establishing a plausible model for our observations, consider the case of the pH 7.0 relaxed-to-rigor situation. The true rigor state is a state in which the S-1 moities extend out to bind with the actin filament at a large angle. In the process of making this contact, the linking element, S-2, tilts up from the thick filament more so than when the fiber is in the relaxed state. A tilt made by the intrinsically anisotropic S-2 element will lead to a decrease in the intrinsic anisotropy due only to orientational change. On the other hand we have evidence that the second type of rigor state, entered from the high pH relaxed state, has a different structure and mechanical rigidity. Here, the actomyosin bond is weaker than the true rigor state, and this rigor bond has much less mechanical stiffness. We have shown that this stretch is due to the breaking of these weaker rigor bonds since the region of overlap decreases upon stretch while the filaments remain at fixed lengths. Optically, this state is characterized by a greatly decreased value of r, when compared with the true rigor state. If we postulate that in this pseudo-rigor state, the binding part of the S-1 elements is oriented at a different angle or at a different location on S-1, from its orientation in the true rigor state, then S-2 will necessarily have to be tilted more from the thick filament axis. Such a crossbridge posture will lead to a further large decrease in r. Reedy and Reedy (32) have recently presented evidence for more than one rigor crossbridge orientation in the insect flight fiber. In that system, the averaged crossbridge structure differs between lead and rear members of double chevrons.

Due to the averaging effects of the optical technique here, we cannot say unequivocally what is actually the disposition of S-1. There can certainly be the possibility that a weaker bond is made when the S-1 shape change has taken place, or when the pseudo-rigor bond is made at a nondistal binding site. Spin-labels and fluorescence labels on S-1 have been used to infer the orientation of the region containing the label. It would be of interest to conduct these probe experiments on the two rigor states that we have uncovered. Furthermore, since optical image reconstruction experiments can discern the existence of two simultaneously existing rigor crossbridge states in the insect flight fiber, that technique should also be able to determine the mass redistributions of the various distinctive populations of rigor crossbridges in frog muscle.

Possible Origin of the Distinct pH-induced Rigor States

Molecular Phase Transition Model. Our studies have shown that if the rigor state of one type has been achieved at any pH value, it is not possible to attain the other rigor state by a simple pH change. The change of the nature of the rigor state can only be achieved if the fiber system is first placed in the relaxed state. This hysteresis has been shown in Fig. 5. Because of the double values of r and Δn_F at a particular rigor pH condition, there could have been a pH-induced molecular phase transition over some segment of the crossbridge that can be prevented by the fiber being in either of the rigor states. In such a model, we postulate that the fiber system can undergo such a phase transition between the pH values of 7.0 and 8.0 when the system is in its relaxed condition. This phase transition would be called upon to determine which of the rigor states the crossbridge can possibly assume. Using enzyme probes, Ueno and Harrington determined that the rigor system at pH 8.0 is more susceptible to enzymatic cleavage than at pH 7.0. Moreover, a region of the myosin rod between the light meromyosin and the S-2 has been shown to be the most susceptible to enzyme action. They further postulate that the region of cleavage susceptibility extends to ~ 10% of the rod dimension. If such a denaturation step reduces the amount of anisotropic element within the fiber, the upper limit of 10% makes it rather difficult to measure by the present method since our observations indicate that upon pH change from 7.0 to 8.15 or above, both r and Δn_F changes are <10% (Table II). Because the cleaving and crosslinking experiments were conducted on myofibril suspensions immersed in pre-conditioned solutions at the various pH values, it is not possible to really say if the myofibrils were in true rigor state or in the pseudo-rigor state. If such a molecular phase transition does take place when pH is raised from 7.0 to above 8.0, as suggested by Ueno and Harrington (19), then the state they determined to be less susceptable to crosslinking must be the pseudo-rigor pH 8.0 state. The pH-induced phase transition makes the fiber more susceptible to cleavage, less susceptible to crosslinking with the myosin thick filament surface, and the rigor bond established is a weaker bond.

Distinctively Different Actomyosin Binding Sites. A second possibility for these rigor states observations is that the normal and weak rigor states are established at different sites. Furthermore, the making of the actomyosin bond itself in either pH state effects a protection of the fiber system from the impacts of a change in pH values. One can perceive of several situations where the rigor bond can prevent the full impact of a solution change. One aspect of this blockage of the effects of the pH environment may be that a rigor state alters the lattice spacing sufficiently to prevent the pH-induced charge effect from affecting the system. Table III suggests that the lattice change is a consequence of the weak-binding state, not its cause. Another possibility is for the rigor bond to physically lock the crossbridge into such an orientation so that pH effects are not felt. A third alternative may be that the presence of nucleotide is needed to create the environment for pH action. In any of these possibilities within the blockage model, one assumes that a true pH 7.0 rigor state is that state we have labeled state *B* of Fig. 5, while the only available state for the fiber placed into rigor at pH 8.15 and higher is that described as state *E* of Fig. 5. When a pH change is made from state *B* to pH 8.15, the state *C* is an artificial state that exists only because the system is already in a rigor configuration. Likewise, the state *F* is an artificial state that resulted from the fiber system not being able to get out of the pseudo-rigor state of *E*, even when the pH of the medium is lowered back to pH 7.0. One test of these three possibilities is the stretch test in the pseudo-rigor states (*E* and *F*). We consider only the artificial state (*F*). Since the ability to stretch is due to the breaking of these weaker rigor bonds, a stretch in the low pH (7.0) state should have released constraints of the lattice change or rigor bond protection and again allow the fiber to go into the true rigor state. This stretch is routinely done to test the mechanical strength of state *F*, and in our experiments this stretch did not cause the fiber to reconfigure into the true rigor state. Given this evidence, the nucleotide-related effect may be more plausible.

Recently, a study by Fink et al. (33) on the effect of ionic strength on rigor force has been reported. In their study, the high μ-state reduced rigor tension appreciably. Furthermore, a "hysteresis" effect was also noted in their study. These authors concluded that the crossbridge bonding positions are influenced by the ionic strength and that these positions of attachment relate to the strengths of the actomyosin bonds. Here, we have demonstrated that pH-related different rigor states also exist, and that these states are structurally different. There may be a relationship between reduced rigor stiffness at high pH and reduced rigor tension at high ionic strength.

The authors are grateful for the expert sample preparations carried out by Ms. Quan You Li.

This work is supported in part through a grant by the National Institutes of Health to Y. Yeh and R. J. Baskin under AM-26817. J. S. Chen is a Visiting Scholar from the People's Republic of China.

Received for publication 6 February 1986 and in final form 7 October 1986.

REFERENCES

1. Cooke, R., M. S. Crowder, C. H. Wendt, V. A. Barnett, and D. D. Thomas. 1984. Muscle crossbridges: do they rotate? *In* Contractile Mechanisms in Muscle. Vol. 1. G. H. Pollack and H. Sugi, editors. Plenum Publishing Corp., New York. 413–423.
2. Yanagida, T. 1981. Angles of nucleotides bound to cross-bridges in glycerinated muscle fibre at various concentrations of ATP, ADP, and AMPPNP detected by polarized flourescence. *J. Mol. Biol.* 146:539–560.
3. Huxley, H. E., R. M. Simmons, A. R. Faruqi, M. Kress, J. Bordas, and M. H. J. Koch. 1981. Millisecond time-resolved changes in x-ray reflections from contracting muscle during rapid mechanical transients, recorded using synchrotron radiation. *Proc. Natl. Acad. Sci. USA.* 78:2297–2301.
4. Huxley, H. E., and M. Kress. 1985. Crossbridge behaviour during muscle contraction. *J. Muscle Res. Cell Motil.* 6:153–161.
5. Brenner, B., M. Schoenberg, J. M. Chalovich, L. E. Greene, and E. Eisenberg. 1982. Evidence for cross-bridge attachment in relaxed muscle at low ionic strength. *Proc. Natl. Acad. Sci. USA.* 79:7288–7291.
6. Brenner, B., L. C. Yu, and R. J. Podolsky. 1984. X-ray diffraction evidence for cross-bridge formation in relaxed muscle fibers at various ionic strengths. *Biophys. J.* 46:299–306.
7. Taylor, K. A., M. C. Reedy, L. Cordova, and M. K. Reedy. 1984. Three-dimensional reconstruction of rigor insect flight muscle from tilted thin sections. *Nature (Lond.).* 310:285–291.
8. Yeh, Y., and R. J. Baskin. 1987. Optical ellipsometry studies on the diffracted orders of single fibers from skeletal muscles. *In* Optical Investigations of Muscle Crossbridges. R. J. Baskin, and Y. Yeh, editors. CRC Press, Boca Raton. In press.
9. Baskin, R. J., Y. Yeh, K. Burton, J. S. Chen, and M. Jones. 1985. Optical depolarization changes in single, skinned muscle fibers: evidence for cross-bridge involvement. *Biophys. J.* 50:63–74.
10. Bragg, W. L., and A. B. Pippard. 1953. The form birefringence of macromolecules. *Acta Crystallogr.* 6:865–867.
11. Yeh, Y., R. J. Baskin, R. A. Brown, and K. Burton. 1985. Depolarization spectrum of diffracted light from muscle fiber. *Biophys. J.* 47:739–742.
12. Sutoh, K., and W. F. Harrington. 1977. Cross-linking of myosin thick filaments under activating and rigor conditions. A study of the radial disposition of cross-bridges. *Biochemistry.* 16:2441–2449.
13. Chiao, Y. C., and W. F. Harrington. 1979. Cross-bridge movement in glycerinated rabbit psoas muscle fibers. *Biochemistry.* 18:959–963.
14. Harrington, W. F. 1971. A mechanochemical mechanism for muscle contraction. *Proc. Natl. Acad. Sci. USA.* 68:685–689.
15. Highsmith, S., C. C. Wang, K. Zero, R. Pecora, and O. Jardetzky. 1982. Bending motions and internal motions in myosin rod. *Biochemistry.*21:1182–1187.
16. Tsong, T. Y., T. Karr, and W. F. Harrington. 1979. Rapid helix-coil transitions in the S-2 region of myosin. *Proc. Natl. Acad. Sci. USA.* 76:1109–1113.
17. Reisler, E., and J. Liu. 1982. Conformational changes in the myosin subfragment-2: effect of pH on synthetic rod filaments. *J. Mol. Biol.* 157:659–669.
18. Applegate, D., and E. Reisler. 1983. Crossbridge release and α-helix-coil transition in myosin and rod minifilaments. *J. Mol. Biol.* 169:455–468.
19. Ueno, H., and W. F. Harrington. 1981. Conformational transition in the myosin hinge upon activation of muscle. *Proc. Natl. Acad. Sci. USA.* 78:6101–6105.
20. Ueno, H., and W. F. Harrington. 1981. Cross-bridge movement and the conformational state of the myosin hinge in skeletal muscle. *J. Mol. Biol.* 149:619–640.
21. Ueno, H., and W. F. Harrington. 1984. An enzyme-probe method to detect structural changes in the myosin rod. *J. Mol. Biol.* 173:35–61.
22. Yeh, Y., M. E. Corcoran, R. J. Baskin, and R. L. Lieber. 1983. Optical depolarization changes on the diffraction pattern in the transition of skinned muscle fibers from relaxed to rigor state. *Biophys. J.* 44:343–351.
23. Fabiato, A., and F. Fabiato. 1979. Calculator programs for computing the composition of the solutions containing multiple metals and ligands used for experiments in skinned muscle cells. *J. Physiol. (Paris).* 75: 463–505.
24. Yeh, Y., and B. G. Pinsky. 1983. Optical polarization properties of the diffraction spectra from single fibers of skeletal muscle. *Biophys. J.* 42:83–90.
25. Irving, M. 1984. Time-resolved measurements of optical retardition in frog isolated muscle fibres. *J. Physiol. (Lond.).* 353:64P.
26. Cassim, J. Y., P. S. Tobias, and E. W. Taylor. 1968. Birefringence of muscle proteins and the problem of structural birefringence. *Biochim. Biophys. Acta.* 168:463–471.
27. Taylor, D. L. 1976. Quantitative studies on the polarization optical properties of striated muscle. I. Birefringence changes of rabbit psoas muscle in the transition from rigor to relaxed state. *J. Cell Biol.* 68:497–511.
28. Rome, E. 1968. X-ray diffraction studies of the filament lattice of striated muscle in various bathing media. *J. Mol. Biol.* 37:331–344.
29. Chen, J. S., R. J. Baskin, K. Burton, and Y. Yeh. 1986. Depolarization spectrum of diffracted light from skinned fibers: ellipsometry measurements of the activated state. *Biophys. J.* 49(2,Pt.2):261a.(Abstr.)
30. Matsubara, I., Y. E. Goldman, and R. M. Simmons. 1984. Changes in the lateral filament spacing of skinned muscle fibres when cross-bridges attach. *J. Mol. Biol.* 173:15–33.
31. Higuchi, H., and Y. Umazume. 1986. Lattice shrinkage with increasing resting tension in stretched, single-skinned fibers of frog muscle. *Biophys. J.* 50:385–389.
32. Reedy, M. K., and M. C. Reedy. 1985. Rigor cross-bridge structure in tilted single filament layers and flared-X formations from insect flight muscle. *J. Mol. Biol.* 185:145–176.
33. Fink, R. H. A., D. G. Stephenson, and D. A. Williams. 1986. Potassium and ionic strength effects on the isometric force of skinned twitch muscle fibres of the rat and toad. *J. Physiol. (Paris).* 370:317–337.